EPJ Web of Conferences **49**, 15008 (2013)
DOI: 10.1051/epjconf/20134915008

Searches for direct supersymmetric gaugino and slepton pair production in final states with leptons with the ATLAS detector

Anders Floderus[1,a] on behalf of the ATLAS Collaboration

[1] *Lund University, Sweden*

Abstract. A search for direct production of supersymmetric gauginos and sleptons in final states with two and three leptons is presented. The two lepton analysis uses 4.7 fb^{-1} of proton-proton collision data at $\sqrt{s}$ = 7 TeV, while the three lepton analysis uses 13 fb^{-1} at $\sqrt{s}$ = 8 TeV. All data were recorded by the ATLAS detector at the Large Hadron Collider. The results are interpreted in the phenomenological minimal supersymmetric Standard Model, as well as simplified models. No significant excess above the Standard Model expectation is observed. Limits on the particle masses are placed at the 95% confidence level. In simplified models, chargino masses are excluded up to 580 GeV.

1 Introduction

Supersymmetry (SUSY) [1–9] postulates that each known particle has a partner whose spin differs by one-half unit with respect to its Standard Model (SM) counterpart. Conservation of R-parity [10–14] implies that SUSY particles can only be produced in pairs, and must eventually decay into some combination of SM particles and the lightest SUSY particle (LSP), which is stable.

Charginos ($\tilde{\chi}_1^\pm$, $\tilde{\chi}_2^\pm$) and neutralinos ($\tilde{\chi}_1^0$, $\tilde{\chi}_2^0$, $\tilde{\chi}_3^0$, $\tilde{\chi}_4^0$), collectively known as gauginos, are the mass eigenstates formed from the linear superposition of the SUSY partners of the Higgs and electroweak gauge bosons. The SUSY partners of the gluons, quarks and leptons are called gluinos ($\tilde{g}$), squarks ($\tilde{q}$) and sleptons ($\tilde{\ell}$). Gauginos and sleptons may dominate SUSY production at the LHC if they are light compared to gluinos and squarks.

A search for direct production of supersymmetric gauginos and sleptons in final states with leptons (electrons or muons) using the ATLAS [15] detector is presented. It is divided into two separate analyses, which are optimized independently. The two lepton analysis looks for two lepton final states, and the three lepton analysis looks for three lepton final states.

2 New Physics Scenarios

The results are interpreted in the framework of the phenomenological minimal supersymmetric Standard Model (pMSSM) [16]. In these models, $\tan\beta$ is set to 6. The gluinos, squarks and left-handed sleptons are taken to be heavy with masses greater than 2 TeV, and the right-handed sleptons are assumed to be degenerate with $m_{\tilde{\ell}_R} = (m_{\tilde{\chi}_2^0} + m_{\tilde{\chi}_1^0})/2$. Signal grids are then generated in the M_2-μ plane for three different values of M_1, where M_1 and M_2 are the gaugino masses and μ is the Higgs mass parameter. In a pMSSM variant referred to as the direct slepton model, left-handed sleptons are lighter with $m_{\tilde{\ell}_L} = m_{\tilde{\ell}_R}$, and all gauginos masses except $\tilde{\chi}_1^0$ are set to 2.5 TeV to favor slepton production.

The results are also interpreted in simplified models [17] where the only free parameters are the masses of the relevant particles, namely $\tilde{\chi}_1^0$, $\tilde{\nu}$, $\tilde{\ell}_L$, $\tilde{\chi}_1^\pm$ and $\tilde{\chi}_2^0$. Right-handed charged sleptons are very heavy with masses above 100 TeV. Two scenarios, both with $m_{\tilde{\chi}_2^0} = m_{\tilde{\chi}_1^\pm}$, are considered. The first scenario includes intermediate sleptons with $m_{\tilde{\nu}} = m_{\tilde{\ell}_L} = (m_{\tilde{\chi}_2^0} + m_{\tilde{\chi}_1^0})/2$. In the second scenario, all slepton masses are above 100 TeV. Signal grids are generated in the $\tilde{\chi}_1^\pm$-$\tilde{\chi}_1^0$ plane.

3 Two Lepton Analysis

The two lepton analysis [18] uses 4.7 fb^{-1} of proton-proton collision data recorded by the ATLAS detector at $\sqrt{s}$ = 7 TeV. The event selection, signal regions, background evaluation method and results are presented.

3.1 Event Selection

Events are selected using a combination of single and double lepton triggers. Each reconstructed triggering lepton must be matched to an online lepton. Jet candidates are reconstructed using the anti-k_t jet algorithm [19] with a distance parameter of 0.4, and are required to satisfy $p_T > 20$ GeV and $|\eta| < 4.5$. Electron candidates must have $p_T > 10$ GeV, $|\eta| < 2.47$, and pass "medium" [20] shower shape and track selection criteria. Muon candidates are required to have matching muon spectrometer and inner detector tracks, and to satisfy $p_T > 10$ GeV and $|\eta| < 2.4$.

[a] e-mail: anders.savonen.floderus@cern.ch

A subset of the object candidates are then selected as signal objects. Signal jets must have $p_{\mathrm{T}} > 30\,\mathrm{GeV}$, $|\eta| < 2.5$ and a jet vertex fraction (JVF) > 0.75. The JVF, which is defined as the fraction of the jet p_{T} that is associated to the primary vertex, is used mainly to reject pileup jets. Signal electrons and muons are required to be isolated, and the electrons must pass "tight" [20] selection criteria.

The missing transverse energy $E_{\mathrm{T}}^{\mathrm{miss}}$ is the magnitude of the missing transverse momentum, $\mathbf{p}_{\mathrm{T}}^{\mathrm{miss}}$. This in turn is the negative of the vector sum of the transverse momentum of all electron and muon candidates, all jets, and all calibrated calorimeter energy clusters with $|\eta| < 4.9$ not associated to such objects. The two lepton analysis makes use of the relative $E_{\mathrm{T}}^{\mathrm{miss}}$, denoted $E_{\mathrm{T}}^{\mathrm{miss,rel.}}$. It is defined as

$$E_{\mathrm{T}}^{\mathrm{miss,rel.}} = \begin{cases} E_{\mathrm{T}}^{\mathrm{miss}} & \text{if } \Delta\phi_{\ell,j} \geq \pi/2 \\ E_{\mathrm{T}}^{\mathrm{miss}} \times \sin\Delta\phi_{\ell,j} & \text{if } \Delta\phi_{\ell,j} < \pi/2 \end{cases}$$

where $\Delta\phi_{\ell,j}$ is the azimuthal angle between the $\mathbf{p}_{\mathrm{T}}^{\mathrm{miss}}$ and the closest signal electron, muon or jet. In events where the momentum of an object has been significantly mismeasured, such that the $\mathbf{p}_{\mathrm{T}}^{\mathrm{miss}}$ is aligned with the object, cutting on $E_{\mathrm{T}}^{\mathrm{miss,rel.}}$ takes into account only the $E_{\mathrm{T}}^{\mathrm{miss}}$ component perpendicular to that object.

3.2 Signal Regions

The two lepton analysis uses four signal regions (SRs), which target different processes as shown in Table 1. An $m_{\ell\ell} > 20\,\mathrm{GeV}$ cut is common to all SRs. Their individual definitions are given in Table 2. The main signal region, SR-m_{T2}, provides sensitivity to both $\tilde{\chi}_1^{\pm}$ and $\tilde{\ell}^{\pm}$ pair production by cutting on the m_{T2} variable [21, 22] defined as

$$m_{\mathrm{T2}} = \min_{\mathbf{q}_{\mathrm{T}}+\mathbf{r}_{\mathrm{T}}=\mathbf{p}_{\mathrm{T}}^{\mathrm{miss}}} \left[\max\left(m_T(\mathbf{p}_{\mathrm{T}}^{\ell_1}, \mathbf{q}_{\mathrm{T}}), m_T(\mathbf{p}_{\mathrm{T}}^{\ell_2}, \mathbf{r}_{\mathrm{T}})\right)\right]$$

where $\mathbf{p}_{\mathrm{T}}^{\ell_1}$ and $\mathbf{p}_{\mathrm{T}}^{\ell_2}$ are the transverse momenta of the two leptons, and $\mathbf{q}_{\mathrm{T}}$ and $\mathbf{r}_{\mathrm{T}}$ are two vectors which satisfy $\mathbf{q}_{\mathrm{T}} + \mathbf{r}_{\mathrm{T}} = \mathbf{p}_{\mathrm{T}}^{\mathrm{miss}}$. m_{T} indicates the transverse mass, $m_{\mathrm{T}} = \sqrt{2E_{\mathrm{T,p}}^{\ell_1} E_{\mathrm{T,q}}(1-\cos\phi)}$, where E_{T} is the transverse energy of a particle and ϕ is the angle between the two particles in the transverse plane.

The SR-OSjveto region is sensitive to $\tilde{\chi}_1^{\pm}$ pair production, and together with SR-SSjveto it also targets three lepton final states where one lepton is either not reconstructed, or falls outside the acceptance of the detector. This provides complementarity to the three lepton analysis. SR-2jets includes a top veto based on the m_{CT} variable [23]. m_{CT} is defined as

$$m_{\mathrm{CT}}(\chi_1, \chi_2) = \left[E_t^2(\chi_1) + E_t^2(\chi_2)\right]^{1/2} - \left[p_T^2(\chi_1) + p_T^2(\chi_2)\right]^{1/2}$$

where χ_i is either a lepton or jet. Events consistent with $t\bar{t}$ kinematics, as described in [24], are rejected.

3.3 Background Evaluation

The main real backgrounds are $t\bar{t}$, single top, Z/γ^*+jets and dibosons (WW, WZ and ZZ). Each background is estimated by defining control regions (CRs) which are dominated by the process of interest, and then extrapolating the number of events observed in the control regions to the signal regions. The number of events $N_{\mathrm{X}}^{\mathrm{CR}}$ in the CR is obtained from data, and the extrapolation is done with a transfer factor $\mathcal{T}$, which is obtained using Monte Carlo (MC). The number of events $N_{\mathrm{X}}^{\mathrm{SR}}$ in the SR is given by

$$N_{\mathrm{X}}^{\mathrm{SR}} = N_{\mathrm{X}}^{\mathrm{CR}} \times \mathcal{T} = N_{\mathrm{X}}^{\mathrm{CR}} \times \left(\frac{N_{\mathrm{X}}^{\mathrm{SR}}}{N_{\mathrm{X}}^{\mathrm{CR}}}\right)_{\mathrm{MC}}.$$

Control regions are defined for top, WW and $Z + X$, which includes Z/γ^*+jets, WZ and ZZ. The definitions are shown in Table 3. The fake background (events containing misidentified jets and real leptons from conversions) is obtained using the matrix method, similarly to what is described in [25]. In SR-SSjveto, there is a "charge-flip" contribution, arising from electrons whose charge is mis-identified after they undergo hard bremsstrahlung with subsequent photon conversion. The charge-flip probability is measured from Z events in data using a likelihood technique [26]. If a signal region or process does not have a control region listed, the background contribution is taken from MC.

Table 1. Process targeted by each two lepton signal region [18].

Targeted Process	Signal Region
Two-lepton Final States	
$\tilde{\ell}^{\pm}\tilde{\ell}^{\mp} \rightarrow (\ell^{\mp}\tilde{\chi}_1^0) + (\ell^{\mp}\tilde{\chi}_1^0)$	SR-m_{T2}
$\tilde{\chi}_1^{\pm}\tilde{\chi}_1^{\mp} \rightarrow (\ell^{\mp}\nu\tilde{\chi}_1^0) + (\ell^{\mp}\nu\tilde{\chi}_1^0)$	SR-m_{T2}, SR-OSjveto
$\tilde{\chi}_2^0\tilde{\chi}_1^{\pm} \rightarrow (\ell^{\mp}\ell^{\mp}\tilde{\chi}_1^0) + (q\bar{q}'\tilde{\chi}_1^0)$	SR-2jets
Three-lepton Final States	
$\tilde{\chi}_2^0\tilde{\chi}_1^{\pm} \rightarrow (\ell^{\mp}\ell^{\mp}\tilde{\chi}_1^0) + (\ell^{\mp}\nu\tilde{\chi}_1^0)$	SR-OSjveto, SR-SSjveto

Table 2. Two lepton signal region definitions. OS (SS) denotes two opposite-sign (same-sign) signal leptons, of same (SF) or different (DF) flavour. Values are in units of GeV. A Z-veto refers to the rejection of events with $m_{\ell\ell}$ within 10 GeV of the Z mass [18]. See text for further details.

SR-	m_{T2}	OSjveto	SSjveto	2jets
charge	OS	OS	SS	OS
flavour	any	any		SF
$m_{\ell\ell}$	Z-veto	Z-veto	-	Z-veto
signal jets	= 0	= 0		≥ 2
signal b-jets	-	-		= 0
$E_{\mathrm{T}}^{\mathrm{miss,rel.}}$	> 40	> 100		> 50
other	$m_{\mathrm{T2}} > 90$	-		m_{CT}-veto

3.4 Results

Good agreement between data and Standard Model expectation is observed in all SRs. Upper limits on the production cross-section times acceptance times efficiency ($\sigma \times \varepsilon \times A$) of new physics are set at the 95% confidence level using the modified frequentist $\mathrm{CL_s}$ prescription [27]. Figure 1 shows the $\tilde{\ell}^{\pm}$ pair production exclusion region in the direct slepton pMSSM. Left-handed slepton masses

Table 3. Two lepton control region definitions. Top is estimated in all OS SRs, WW in SR-OSjveto and $Z + X$ in all SF channels of the OS SRs. When the CRs use different cuts for each SR, they are given as a comma separated list in the order of SR-OSjveto, SR-2jets, SR-m_{T2} [18]. Values are in units of GeV.

Selection	top	WW	$Z + X$
$m_{\ell\ell}$	Z-veto	Z-veto	Z-window
signal jets	≥ 2	=0	$= 0, \geq 2, \geq 0$
signal b-jets	≥ 1	=0	$\geq 0, = 0, \geq 0$
$E_T^{\rm miss,rel.}$	$> 100, 50, 40$	70–100	$> 100, 50, 40$
other	-	-	-, m_{CT}-veto, -

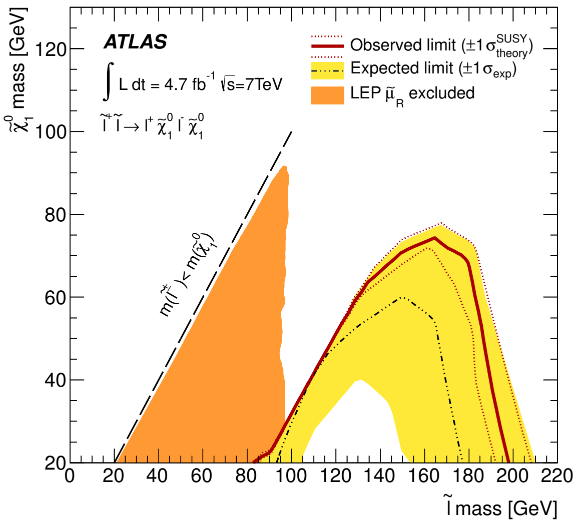

Figure 1. Observed and expected 95% CL limit contours for $\tilde{\ell}^{\pm}$ pair production in the direct slepton pMSSM. The expected and observed limits are calculated without signal cross-section uncertainty taken into account. The yellow band is the $\pm 1\sigma$ experimental uncertainty on the expected limit (black dashed line). The red dotted band is the $\pm 1\sigma$ signal theory uncertainty on the observed limit (red solid line) [18]. Illustrated also is the LEP limit [28] on the mass of the right-handed smuon, $\tilde{\mu}_R$.

between 85 and 195 GeV are excluded for a 20 GeV neutralino. Figure 2 shows the $\tilde{\chi}_1^{\mp}$ pair production exclusion region in the simplified model. Chargino masses between 110 and 340 GeV are excluded for a 10 GeV neutralino.

The 4.7 fb^{-1} two lepton $\tilde{\chi}_2^0\tilde{\chi}_1^{\pm}$ limits are not shown as they are superseded by the more recent 13 fb^{-1} three lepton $\tilde{\chi}_2^0\tilde{\chi}_1^{\pm}$ limits, which are presented in Section 4.4.

4 Three Lepton Analysis

The three lepton analysis [29] uses 13 fb^{-1} of proton-proton collision data recorded by the ATLAS detector at $\sqrt{s} = 8$ TeV. The event selection, signal regions, background evaluation method and results are presented.

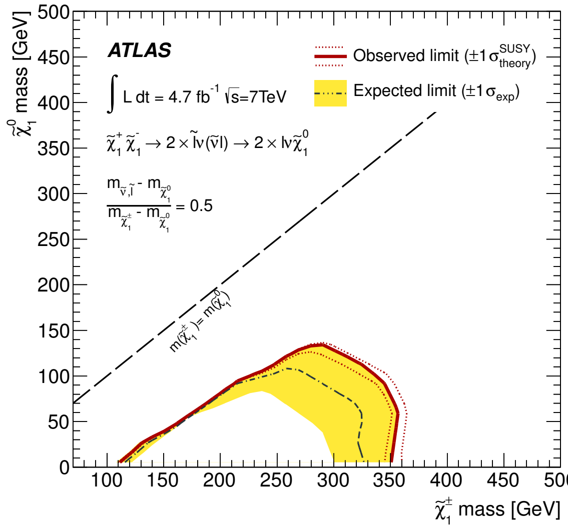

Figure 2. Observed and expected 95% CL limit contours for $\tilde{\chi}_1^{\pm}$ pair production in the simplified model scenario with intermediate sleptons [18]. The color coding is the same as in Figure 1.

4.1 Event Selection

Events are selected using an inclusive set of double-lepton triggers. Each reconstructed triggering lepton must be matched to an online lepton. The jet, electron and muon candidate definitions as well as the $E_T^{\rm miss}$ definition are the same as in Section 3.1. A subset of the object candidates are selected as signal objects. Signal jets must have $|\eta| < 2.5$ and a JVF > 0.5. Signal electrons and muons are required to be isolated, and the electrons must pass the "tight" selection criteria.

4.2 Signal Regions

The three lepton analysis targets $\tilde{\chi}_2^0\tilde{\chi}_1^{\pm}$ production, and uses three SRs corresponding to various $\tilde{\chi}_2^0$ decay modes. Their definitions are shown in Table 4. SR1a and SR1b target $\tilde{\chi}_2^0$ decays that proceed via sleptons and off-shell Z bosons, while SR2 targets on-shell Z bosons. Common to all these decay modes is the presence of a pair of same-flavor opposite-sign (SFOS) leptons in the final state. All SRs require exactly three leptons, including an SFOS pair with $m_{\rm SFOS} > 12$ GeV. The transverse mass is defined as $m_T = \sqrt{2 \cdot E_T^{\rm miss} \cdot p_T^{\ell} \cdot (1 - \cos\Delta\phi_{\ell, E_T^{\rm miss}})}$ where ℓ denotes the lepton that is not part of the pair forming the best Z-candidate. SR1b is a subset of SR1a, designed to increase sensitivity to models where the mass splitting between $\tilde{\chi}_1^0$ and the other gauginos is large.

4.3 Background Evaluation

As in the two lepton analysis, the fake background is obtained using the matrix method. The main real background comes from WZ, and is estimated using a refined version

Table 4. Three lepton signal region definitions [29].

Selection	SR1a	SR1b	SR2
Targeted $\tilde{\chi}_2^0$ decay	$\tilde{\ell}^{(*)}$ or Z^*		on-shell Z
$\lvert m_{\mathrm{SFOS}} - m_Z \rvert$	$> 10\,\mathrm{GeV}$		$< 10\,\mathrm{GeV}$
Number of b-jets	0		any
$E_{\mathrm{T}}^{\mathrm{miss}}$	$> 75\,\mathrm{GeV}$		$> 120\,\mathrm{GeV}$
m_{T}	any	$> 110\,\mathrm{GeV}$	$> 110\,\mathrm{GeV}$
p_{T} of leptons	$> 10\,\mathrm{GeV}$	$> 30\,\mathrm{GeV}$	$> 10\,\mathrm{GeV}$

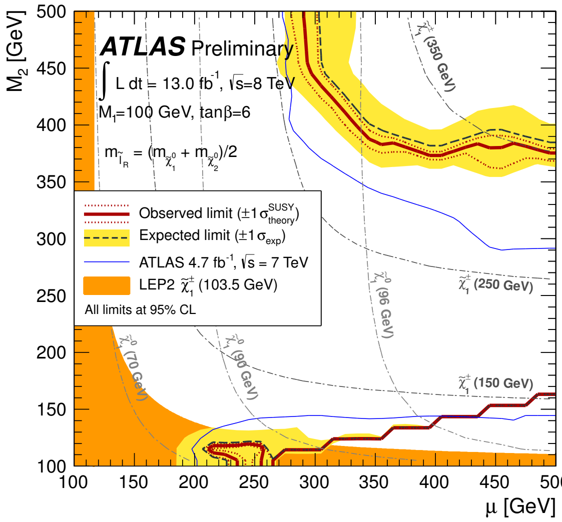

Figure 3. Observed and expected 95% CL limit contours for $\tilde{\chi}_2^0\tilde{\chi}_1^\pm$ production in the pMSSM for $M_1 = 100\,\mathrm{GeV}$. The expected and observed limits are calculated without signal cross-section uncertainty taken into account. The yellow band is the $\pm 1\sigma$ experimental uncertainty on the expected limit (black dashed line). The red dotted band is the $\pm 1\sigma$ signal theory uncertainty on the observed limit (red solid line) [29]. The blue lines correspond to the 7 TeV limits from the combination of the two lepton and three lepton analyses [30]. The LEP2 limit corresponds to the limit on the $\tilde{\chi}_1^\pm$ mass in [31] as transposed to this pMSSM plane.

of the method described in Section 3.3. This method includes a WZ normalization factor that takes into account differences between data and MC in the CR, as well as a non-negative signal contribution in the SR. These two parameters are kept floating and fitted simultaneously in the CR and SR to set limits on the cross section for new physics while correctly propagating the uncertainty on the normalization. The WZ CR requirements are: exactly three leptons with $p_{\mathrm{T}} > 20\,\mathrm{GeV}$, one SFOS lepton pair, a Z candidate, $50 < E_{\mathrm{T}}^{\mathrm{miss}} < 75\,\mathrm{GeV}$, a b-veto, and $50 < m_{\mathrm{T}} < 110\,\mathrm{GeV}$. Remaining backgrounds are taken from MC.

4.4 Results

Good agreement between data and Standard Model expectation is observed in all SRs. Upper limits on the production cross-section times acceptance times efficiency ($\sigma \times \varepsilon \times A$) of new physics are set at the 95% confidence level using the modified frequentist CL$_s$ prescription.

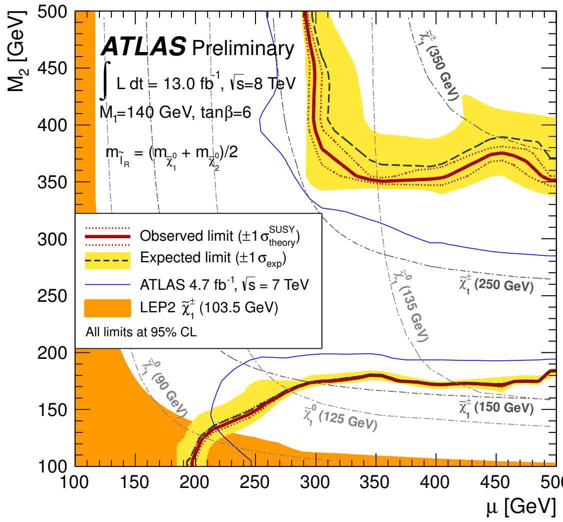

Figure 4. Observed and expected 95% CL limit contours for $\tilde{\chi}_2^0\tilde{\chi}_1^\pm$ production in the pMSSM for $M_1 = 140\,\mathrm{GeV}$ [29]. The color coding is the same as in Figure 3.

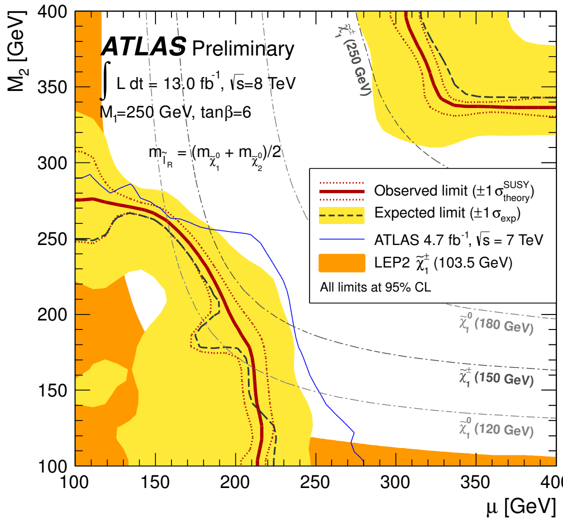

Figure 5. Observed and expected 95% CL limit contours for $\tilde{\chi}_2^0\tilde{\chi}_1^\pm$ production in the pMSSM for $M_1 = 250\,\mathrm{GeV}$ [29]. The color coding is the same as in Figure 3.

Figure 3, 4 and 5 shows the $\tilde{\chi}_2^0\tilde{\chi}_1^\pm$ production exclusion region in the pMSSM for $M_1 = 100\,\mathrm{GeV}$, $M_1 = 140\,\mathrm{GeV}$ and $M_1 = 250\,\mathrm{GeV}$, respectively. Figure 6 and 7 show the $\tilde{\chi}_2^0\tilde{\chi}_1^\pm$ exclusion region in the simplified model scenarios with and without intermediate sleptons. Chargino masses are excluded up to 580 GeV and 300 GeV, respectively.

5 Summary

A search for direct production of supersymmetric gauginos and sleptons in final states with leptons has been presented. The results are interpreted in the pMSSM and simplified models. No significant excess above the Standard Model expectation has been observed. In the simpli-

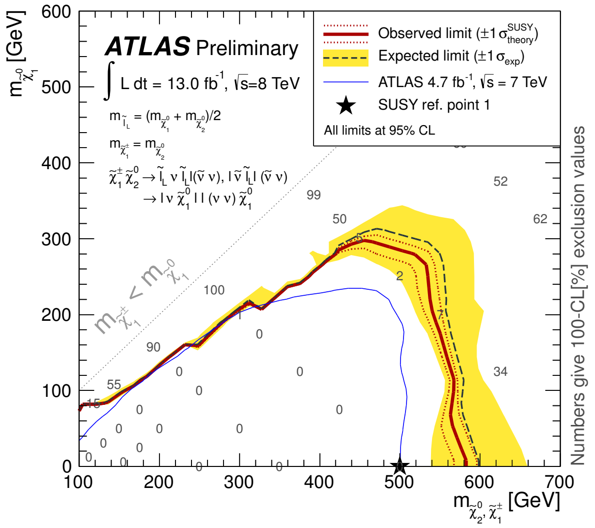

Figure 6. Observed and expected 95% CL limit contours for $\tilde{\chi}_2^0\tilde{\chi}_1^\pm$ production in the simplified model scenario with intermediate sleptons. The 100-CL[%] value is shown for each of the simulated model points [29]. The blue line corresponds to the 7 TeV limits from the three lepton analysis [30]. Remaining color coding is the same as in Figure 3.

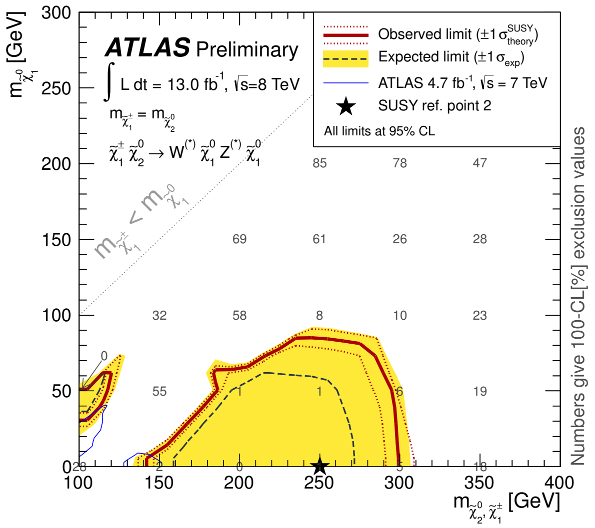

Figure 7. Observed and expected 95% CL limit contours for $\tilde{\chi}_2^0\tilde{\chi}_1^\pm$ production in the simplified model scenario without intermediate sleptons. The 100-CL[%] value is shown for each of the simulated model points [29]. The blue line corresponds to the 7 TeV limits from the three lepton analysis [30]. Remaining color coding is the same as in Figure 3.

fied model scenarios with and without intermediate sleptons, chargino masses are excluded up to 580 GeV and 300 GeV, respectively.

References

[1] Miyazawa, H., Prog. Theor. Phys. **36 (6)**, 1266-1276 (1966)

[2] Ramond, P., Phys. Rev. **D3**, 2415-2418 (1971)

[3] Golfand, Y. A. et al., JETP Lett. **13**, 323-326 (1971)

[4] Neveu, A. and Schwarz, J. H., Nucl. Phys. **B31**, 86-112 (1971)

[5] Neveu, A. and Schwarz, J. H., Phys. Rev. **D4**, 1109-1111 (1971)

[6] Gervais, J. L. and Sakita, B., Nucl. Phys. **B34**, 632-639 (1971)

[7] Volkov, D. V. and Akulov, V. P., Phys. Lett. **B46**, 109-110 (1973)

[8] Wess, J. and Zumino, B., Phys. Lett. **B49**, 52 (1974)

[9] Wess, J. and Zumino, B., Nucl. Phys. **B70**, 39-50 (1974)

[10] Fayet, P., Phys. Lett. **B64**, 159 (1976)

[11] Fayet, P., Phys. Lett. **B69**, 39-50 (1977)

[12] Farrar, G. R. and Fayet, P., Phys. Lett. **B76**, 575-579 (1978)

[13] Fayet, P., Phys. Lett. **B84**, 416 (1979)

[14] Dimopoulos, S. and Georgi, H., Nucl. Phys. **B193**, 150 (1981)

[15] ATLAS Collaboration, JINST **3**, S08003 (2008)

[16] Djouadi, A. et al., Comput. Phys. Commun. **176**, 426-455, (2007)

[17] Alwall, J. et al., Phys. Rev. **D79**, 075020, (2009)

[18] ATLAS Collaboration, arXiv:1208.2884 [**hep-ex**]

[19] Cacciari, M., Salam, G. P. and Soyez, G., JHEP **04**, 063 (2008)

[20] ATLAS Collaboration, JHEP **12**, 060 (2010)

[21] Barr, A., Lester, C. and Stephens, P., J.Phys.G **G29**, 2343-2363 (2003)

[22] Lester, C. G. and Summers, D. J., Phys. Lett. **B463**, 99-103 (1999)

[23] Tovey, D. R., JHEP **04**, 034 (2008)

[24] Polesello, G. and Tovey, D. R., JHEP **03**, 030 (2010)

[25] ATLAS Collaboration, Eur. Phys. J. **C71**, 1577 (2011)

[26] ATLAS Collaboration, JHEP **04**, 069 (2012)

[27] Read, A. L., J. Phys. G **G28**, 2693-2704 (2002)

[28] LEP SUSY Working Group (ALEPH, DELPHI, L3, OPAL), Notes LEPSUSYWG/01-03.1 and 04-01.1

[29] ATLAS Collaboration, ATLAS-COM-CONF-2012-192, https://cds.cern.ch/record/1493493

[30] ATLAS Collaboration, arXiv:1208.3144 [**hep-ex**]

[31] Nakamura, K. and Particle Data Group, J. Phys. G: Nucl. Part. Phys. **37**, 075021 (2010)